

Original Article	A Light and Electron Microscopic Study on the Role of Granulocyte Colony Stimulating Factor Therapy on Carbon Tetrachloride Induced Lung Fibrosis in Adult Male Albino Rats <i>Mona H. Mohammed Ali, Omayma M. Mahmoud, Nermine S. Nosseir and Hala M. Ebaid*</i> <i>Anatomy Department, Faculty of Medicine and * Zoology Department , Faculty of Science, Suez Canal University</i>
-------------------------	--

ABSTRACT

Background: Pulmonary fibrosis is a serious fatal form of interstitial lung diseases and unfortunately no effective therapy exists. Hematopoietic Stem Cells (HSCs) have been used for hematological reconstitution for many years. Recently, however, homing and engraftment of HSCs in damaged non-hematopoietic organs have been observed and were suggested to contribute to the wound healing process.

Aim of the work: To test whether the chemokine Granulocyte Colony Stimulating Factor (G-CSF) could promote lung repair and recovery after fibrosis in adult male rats.

Materials and Methods: A total of eighty adult male rats were divided randomly into four groups: Group (I): Control group. Group (II): Carbon tetrachloride-treated group where the animals were injected with carbon tetrachloride (CCL4) intraperitoneally at a dose of 0.6 mg /Kg B.W daily for 14 consecutive days and then were subdivided into two subgroups: Group (a) in which the animals were sacrificed 24 hours after the last administration and Group (b) in which the animals were sacrificed 14 days after the last administration. Group (III): G-CSF+carbon tetrachloride-treated group where the animals were injected with carbon tetrachloride (CCL4) intraperitoneally at a dose of 0.6 mg /Kg B.W daily for 14 consecutive days and then G-CSF (Neupogen) in a dose of (100 µg/kg/day) subcutaneously for 5 consecutive days and the animals were sacrificed 14 days after the last administration. Group (IV): G-CSF-treated group where the animals were injected with G-CSF (Neupogen) in a dose of (100 µg/kg/day) subcutaneously for 5 consecutive days and the animals were sacrificed 14 days after the last administration. The lungs were prepared and processed for light and electron microscopic examination.

Results: It has been found that rats treated with carbon tetrachloride showed extensive congestion and rupture of most of the blood capillaries, marked thickening of the interalveolar septa, marked narrowing, distortion and occlusion in most of the air spaces. A large number of inflammatory cells in the pulmonary tissue and marked increase in the amount of collagen fibers were also observed. The results obtained from the group of rats treated with both G-CSF+carbon tetrachloride revealed marked reduction in the above mentioned pathological changes in the lungs.

Conclusion: Although the exact mechanisms are not wholly understood, there is evidence that bone marrow-derived stem cells are able to contribute to promote healing of lung fibrosis.

Key Words: Carbon tetrachloride, lung fibrosis, G-CSF, rats.

Corresponding Author: Dr. Mona H. Mohammed Ali, Anatomy Department, Faculty of Medicine, Suez Canal University, Ismailia, Egypt, Email: hararh2002@yahoo.com, Mobile: 0106823131.

INTRODUCTION

Respiratory diseases remain one of the main causes of morbidity and mortality in the world (Loebinger & Janes, 2007). Pulmonary fibrosis is a serious restrictive and severe progressive lung disorder (Taylor et al., 2003) that may occur idiopathically or as a complication of many diseases and unfortunately has a poor

prognosis (Zhang et al., 2007). Mehrnaz et al. (2007) demonstrated that pulmonary fibrosis is a chronic, progressive and often fatal form of interstitial lung disease that is characterized by injury with loss of lung epithelial cells and abnormal tissue repair, resulting in destruction of the normal functional tissue, abnormal accumu-

lation of fibroblasts and myofibroblasts, deposition of extracellular matrix and distortion of lung architecture which results in respiratory failure. Furthermore, it is a devastating disease for which no effective therapy exists (Mason *et al.*, 1999; Gross & Hunninghake, 2001).

Interest has increased to the possibility of optimizing the repair of the lung with manipulation of stem cells. Embryonic and adult stem cells have been suggested as possibilities. Adult stem cells have been thought of having limited differentiation ability and to be organ specific. However, a series of exciting reports have suggested that adult bone marrow-derived stem cells may have more plasticity and are able to differentiate into bronchial and alveolar epithelium, vascular endothelium and interstitial cell types, making them prime candidates for repair (Blau *et al.*, 2001; Loebinger & Janes, 2007). Granulocyte colony stimulating factor (G-CSF), a 20-kDa glycoprotein, is known to induce granulopoiesis (Clark & Kamen 1987) to produce earlier healing by acting on the inflammatory system (Gough *et al.*, 1997 & Edmonds *et al.*, 2000) and to have immuno-regulatory properties in addition to inducing cell differentiation (Hartung, 1999). Sehara *et al.* (2007) demonstrated that administration of G-CSF is known to mobilize hematopoietic stem cells (HSCs) from bone marrow into peripheral blood and to stimulate the proliferation of neutrophil progenitors. Moreover, Orlic *et al.* (2001) reported that the peripheral blood-derived cells from HSCs have been used in place of bone marrow cells for the regeneration of non-hematopoietic tissue. Additionally, G-CSF has been used extensively in the treatment for bone marrow reconstruction and stem cell mobilization (Weaver *et al.*, 1993). Therefore, especially in the environment where intense inflammation occurs, it is possible that G-CSF affects the healing process by modulating the inflammatory reaction and collagen synthesis (Sehara *et al.*, 2007).

In this study, a rat model of lung fibrosis was used to test whether the chemokine G-CSF could promote lung repair and recovery after fibrosis, which would provide a basis for the development of a non-invasive therapy for pulmonary fibrosis.

MATERIALS AND METHODS

Healthy, adult male albino rats weighing 200 ± 10 g were used in this study. They were acclimatized for one week prior to the experiment. Rats were housed five per cage in stainless steel cages and fully ventilated room at room temperature. They were maintained on a photoperiod of 12 h light/12 h dark and fed a standard laboratory pelleted food and water ad libitum. All experimental procedures and animal maintenance were conducted in accordance with the accepted standards of animal care. Rats were divided randomly into 4 groups, each included 20 rats:

- **Group I [Control group]:** The animals received intraperitoneal injection of 1.5 ml of sterile distilled water daily for 14 consecutive days and then were subdivided into two subgroups: Group (a) in which the animals were sacrificed 24 hours after the last administration (10 rats) and Group (b) in which the animals were sacrificed 14 days after the last administration (10 rats).
- **Group II [Carbon tetrachloride-treated group]:** The animals were injected intraperitoneally with carbon tetrachloride (CCL4) at a dose of 0.6 mg/Kg B.W daily for 14 consecutive days (Zakareya *et al.*, 2004) and were subdivided into two subgroups: Group (a) in which the animals were sacrificed 24 hours after the last administration (10 rats) and Group (b) in which the animals were sacrificed 14 days after the last administration (10 rats).
- **Group III: [G-CSF+carbon tetrachloride-treated group]:** The animals were injected intraperitoneally with carbon tetrachloride (CCL4) at a dose of 0.6 mg/Kg B.W daily for 14 consecutive days (Zakareya *et al.*, 2004) and then G-CSF (Neupogen) in a dose of (100 μ g/kg/day) subcutaneously for 5 consecutive days and the animals were sacrificed 14 days after the last administration (Ortiz *et al.*, 2003).

- **Group (IV) [G-CSF-treated group]:** The animals were injected with G-CSF (Neupogen) in a dose of (100 µg/kg/day) subcutaneously for five consecutive days and the animals were sacrificed 14 days after the last administration (Ortiz et al. 2003).

CCl4 was obtained from ADWIC Co, Egypt, and used as 50% solution in olive oil. G-CSF (Neupogen) was obtained from La Roche LTD, Basel and Swizerland.

The animals were sacrificed by decapitation and carefully dissected. The lungs were removed and carefully examined. The right lungs were fixed in 10% neutral buffered formalin solution for 24 hours, dehydrated in a graded ethanol series and processed for paraffin embedding for light microscopic study. Serial sections (four µm thick) were prepared and stained with: Hematoxylin and Eosin (Hx&E) and Masson's trichrome staining for studying and comparing the different components of the alveolar septa of the lung. The left lungs were processed for electron microscopic examination. The lungs were carefully dissected and divided into small pieces that were fixed in buffered 2.5% glutaraldehyde for two hours (two changes) and post fixed in 1% osmic tetroxide for electron microscopic studies. Dehydration was performed in ascending grades of alcohol and embedded in epoxy resin. One micrometer thick sections were cut, stained with toluidine blue and examined with light microscope. Ultrathin sections were cut using MT 600-XL RMC ultratome and stained with uranyl acetate, lead citrate, examined with a Joel 1200 EX 11 Transmission Electron Microscope, at the Faculty of Science, Ain Shams University and photographed under different magnification.

Morphometric Study:

By the aid of the Leica Q 500 image system [LICA Microsystem Corporation, England] the degree of morphological involvement in lung fibrosis was determined using light microscope. The following parameters were chosen as indicative of pathological damage to the lung: Thickness of the alveolar septum, number and degree of alveolar septal cellularity. Each parameter was determined in five different rats in three sections from each animal.

Statistical Analysis:

All data were expressed as mean±SE and compared by one-way analysis of variance (ANOVA). The interaction in all groups was analyzed using SNK-*q* in SPSS 12.0. Differences in values were considered significant if $P < 0.05$.

RESULTS

- **Group I [control group] (a&b):**

Light microscopic examination of the lung tissues revealed normal lung architecture. The lungs showed a gland-like structure containing bronchioles and alveolar spaces. The bronchioles were lined with simple columnar ciliated cells and were supported by connective tissue and the alveolar spaces were separated by interalveolar septa. These septa appeared thin, clear and were covered on both sides with flattened epithelium and contained numerous capillaries. In some sites, the basement membrane of the alveoli appeared fused with that of capillaries, while in other areas they were separated by a space containing mononuclear cells. Large rounded cells (alveolar phagocytes) were occasionally seen bulging from the alveolar walls into the alveolar spaces (Fig. 1). Stained semithin sections with toluidine blue revealed that most of the alveolar epithelium was covered by large, flattened squamous cells; type I pneumocytes while type II pneumocytes occupied a much smaller proportion of the alveolar surface (Fig. 2). Type I pneumocytes constituted about (32.17%) of the total alveolar epithelial cells, while type II pneumocytes constituted about (67.83%) of the total alveolar epithelial cells (Table 1). Masson's trichrome stained sections showed that collagen fibers appeared as minimal amounts of thin bundles around the walls of the bronchioles and fewer amounts in the interalveolar septa (Fig. 3).

The ultrastructure results revealed empty and clear alveolar spaces. The type II pneumocytes appeared large with large rounded centrally-placed nucleus showing peripheral condensed chromatin. Short apical blunt-ended microvilli with variable size were seen projecting from their luminal border into the alveolar lumen. Small

dense mitochondria and large number of lamellar bodies filled with surfactant were also detected in the cytoplasm of most cells (Figs. 4, 5). Type I pneumocytes showed flattened nucleus and attenuated cytoplasm (Figs. 6, 7). Rarely, alveolar macrophages were seen in the lumen of the alveoli. Cross and longitudinal sections of collagen fibers were also observed in the interalveolar septa. Normal intact blood-air barrier formed from cytoplasm of type I pneumocyte, cytoplasm of endothelial cells of capillary, fused basal lamina of pneumocyte type I and endothelial cells of capillary was seen (Fig. 8).

- **Group II [carbon tetrachloride-treated group] (a&b):**

Light microscopic examination of the lung specimens showed marked narrowing, distortion and occlusion of nearly all alveolar spaces together with marked congestion and rupture of many capillaries combined with extravasation of red blood cells inside the alveolar spaces. These narrow alveolar spaces showed a large number of macrophages containing phagocytic vacuoles together with degenerated and detached parts of cells in some regions. Marked increase in the thickness of the interalveolar septa was detected. The thickened septa showed mononuclear cellular infiltration consisting mainly of macrophages, lymphocytes and fibroblasts (Figs. 9-11). The mean thickness of the interalveolar septa was 3.848 ± 1.049 mm. This thickness showed a statistically highly significant increase when compared to the control group. Hypocellularity in type I and II pneumocytes were observed. The mean of the total cellularity of the interalveolar septa was 64.20 ± 3.56 . Type I pneumocytes constituted 29.5% of the total alveolar epithelium cells, while type II pneumocytes constituted about 70.5% of the total alveolar epithelium cells. This observed hypocellularity in both type I and type II pneumocytes were proven to be statistically highly significant decrease when compared to the control group (Table 1). Masson's trichrome stained sections revealed marked increase in the amount of collagen fibers around the bronchioles, in the interalveolar septa and in the pulmonary blood vessels (Fig. 12).

The ultrastructure study of the lung tissues of the rats showed narrow alveolar spaces with ac-

cumulation of inflammatory cells inside them. Some cellular debris, alveolar macrophage, detached parts of cells and extravasated red blood cells were also seen within the alveolar spaces together with multiple vacuolations of the cytoplasm (Figs. 13, 14). Almost all type II pneumocytes showed loss of microvilli, multiple vacuolations of the cytoplasm and swelling of the lamellar bodies. Shrinkage of some cells with loss of tight junctions between them were observed in some regions. Obvious increase in the amount of longitudinally and circularly oriented collagen fibers were also seen (Figs. 15, 16). Type I pneumocytes showed also vacuolations, lightly stained nucleus and infiltration of glycogen. Loss of tight junctions between type I pneumocytes was evident in most regions (Fig. 17). Rupture of the blood-air barrier with extravasation of blood cells into the alveolar spaces were evident (Fig. 18).

- **Group III [G-CSF+carbon tetrachloride-treated group]:**

Light microscopic examination showed a gland-like appearance composed of bronchioles and alveolar spaces. The bronchioles were lined with columnar cells and were supported by connective tissue and the alveolar spaces were separated by interalveolar septa. These septa were covered on both sides with flattened epithelium with many capillaries. Mean thickness of the interalveolar septum was 0.441 ± 0.075 mm that showed a highly statistically significant decrease when compared to the carbon-tetrachloride treated group (Table 1). Stained semithin sections with toluidine blue revealed that most of the alveolar epithelium was covered by large, flattened squamous cells (type I pneumocytes), while type II pneumocytes occupied a much smaller proportion of the alveolar surface (Figs. 19, 20). The mean of the total cellularity of the interalveolar septa was 110.20 ± 12.62 . This mean of cellularity was proven to be statistically significant increase when compared to both the control and the carbon tetrachloride-treated groups (Table 1). Type I pneumocytes constituted about 29.5% of the total alveolar epithelium cells that proved to be statistically insignificant in comparison to the control group, but highly significant increase when compared to the carbon tetrachloride-treated group

(Table 1). Type II pneumocytes constituted about 70.5% of the total alveolar epithelium cells. This value was proved to be statistically significant decrease in comparison to the control group and highly statistically significant increase in comparison to the carbon tetrachloride-treated group (Table 1). Masson's trichrome stained sections revealed a moderate amount of collagen fibers in the interalveolar septa and around the bronchioles (Fig. 21).

The ultrastructure study of the lung tissues of the rats showed slightly congested blood capillaries and the lamina of most capillaries were empty without any inclusions in most regions. Occasional cell fragments in focal areas were detected. Type II pneumocytes displayed normal short apical microvilli, cytoplasmic organelles with large rounded centrally-placed nucleus with peripheral condensed chromatin. The mitochondria were detected with well preserved outer and inner mitochondrial membranes. No vaculation of the cytoplasm was observed (Fig. 22). Type I pneumocytes appeared normal with their flattened nuclei and attenuated cyto-

plasm (Fig. 23). Few amount of collagen fibers was observed. Type II pneumocytes showing features of turnover to type I pneumocytes were observed. These features were in the form of changing nucleus from large rounded to flat appearance combined with losing both microvilli and lamellar bodies (Fig. 24). The blood-air barrier appeared intact and made up from cytoplasm of type I pneumocytes, cytoplasm of endothelial cells of continuous capillary, fused basal lamina of type I pneumocytes and endothelial cells of the capillary (Fig. 25).

• **Group IV [G-CSF -treated group]:**

Light microscopic examination of the lung tissues revealed a picture similar to that found in the control group. Mean thickness of the interalveolar septa and mean cellularity were very near to those in the control group. Stained semithin sections with toluidine blue gave a picture similar to that found in the control group. Masson trichrome stained sections revealed a minimal amount of collagen fibers in the interalveolar septa and around the bronchioles. The ultrastructure study of lung tissue revealed a picture similar to that detected in the control group.

Table 1: Morphometric characteristics in the different groups.

	Type I pneumocytes Mean±SE	Type II pneumocytes Mean±SE	Total cellularity Mean±SE	Septal thickness (mm) Mean±SE
Group I [Control group] (a&b)	7.40±1.67 (32.17%)	15.60±1.14 (67.83%)	94.20±6.14	0.366±0.139
Group II [carbon tetrachloride- treated group] (a&b)	3.60±1.14*♦ ↓ (29.5%)	8.60±1.26*♦ ↓ (70.5%)	64.20±3.56*♦ ↓	3.848±1.049*♦ ↑
Group III: [G-CSF+carbon tetrachloride- treated group]	5.60±1.14* ↓ (29.5%)	13.40±1.17* ↓ (70.5%)	110.20±12.62* ↑	0.441±0.075
Group IV [G-CSF- treated group]	7.30±1.01 (32.01%)	15.50±1.02 (77.09%)	95.00±5.09	0.365±0.437

P < 0.05

* Significant in comparison to the control group.

♦ Significant in comparison to the G-CSF+carbon tetrachloride-treated group.

Decrease ↓ Increase ↑

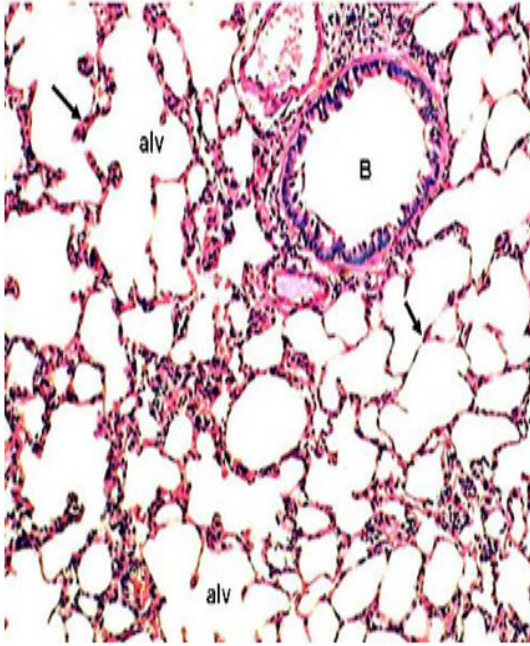


Fig.1: A photomicrograph of a section in the lung of a rat of the control group showing normal lung architecture. Note the alveolar space (alv), respiratory bronchiole (B) and interalveolar septum (arrow).
Hx.&E.; X400

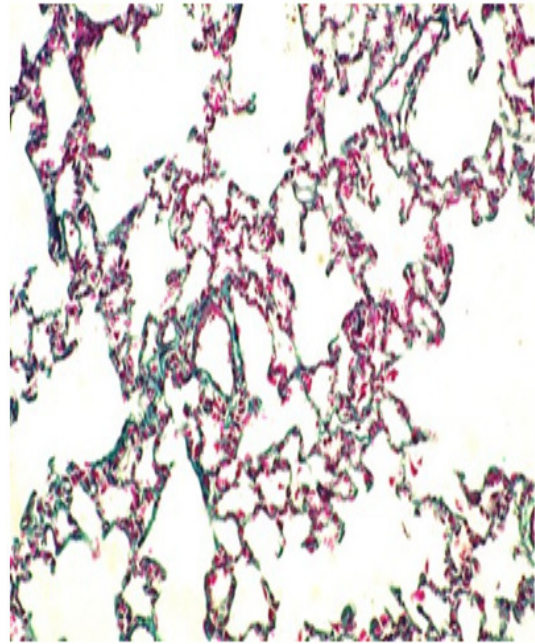


Fig. 3: A photomicrograph of a section in the lung of a rat of the control group showing few amount of green collagen fibers in the interalveolar septa.
Masson's trichrome; X400

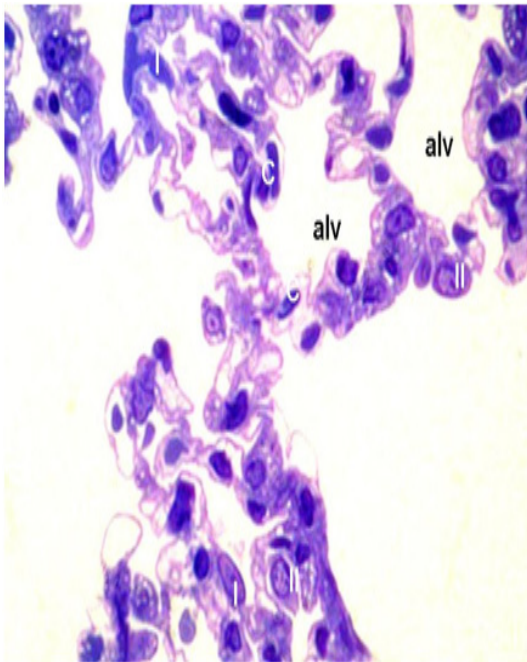


Fig. 2: A photomicrograph of a section in the lung of a rat of the control group showing normal cellularity, type I pneumocytes (I), type II pneumocytes (II), alveolar space (alv) and red blood cell inside capillary lumen (C).
Toluidine blue; X1000

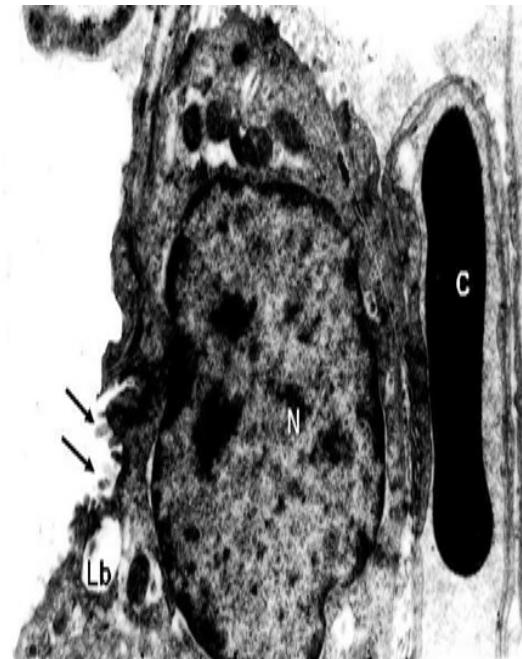


Fig. 4: An electron photomicrograph in the lung of a rat of the control group showing type II pneumocytes with normal lamellar body (Lb), nucleus (N), microvilli (arrows) and red blood cell inside capillary lumen (C).
Uranyl acetate and Lead citrate; X 7,500

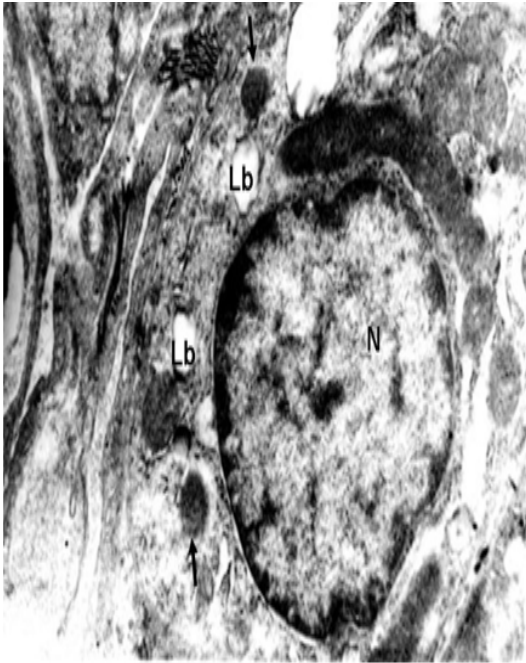


Fig. 5: An electron photomicrograph in the lung of a rat of the control group showing type II pneumocytes with lamellar body (Lb), nucleus (N) and mitochondria (arrow).
Uranyl acetate and Lead citrate ; 10,000

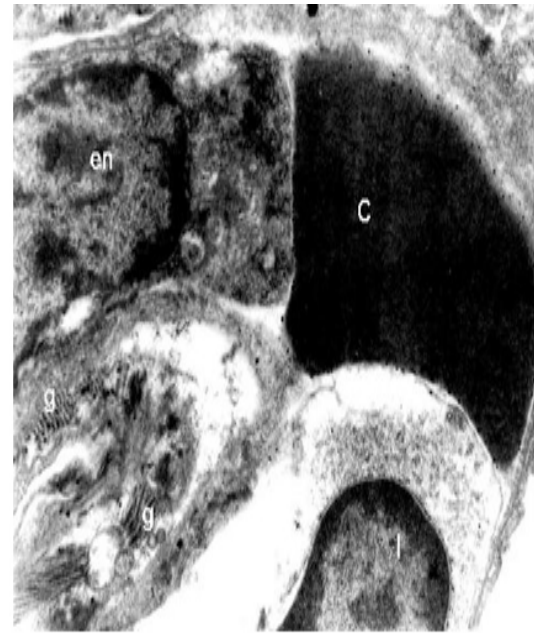


Fig. 7: An electron photomicrograph in the lung of a rat of the control group showing nucleus of type I pneumocytes (I), nucleus of endothelial cell of capillary (en), red blood cell inside capillary lumen (C) and few amount of collagen fibers (g).
Uranyl acetate and Lead citrate; X 12,000



Fig. 6: An electron photomicrograph in the lung of a rat of the control group showing type I pneumocytes with nucleus (N), few amount of collagen fibers (g) and normal intact blood air barrier (arrows).
Uranyl acetate and Lead citrate; X 10,000

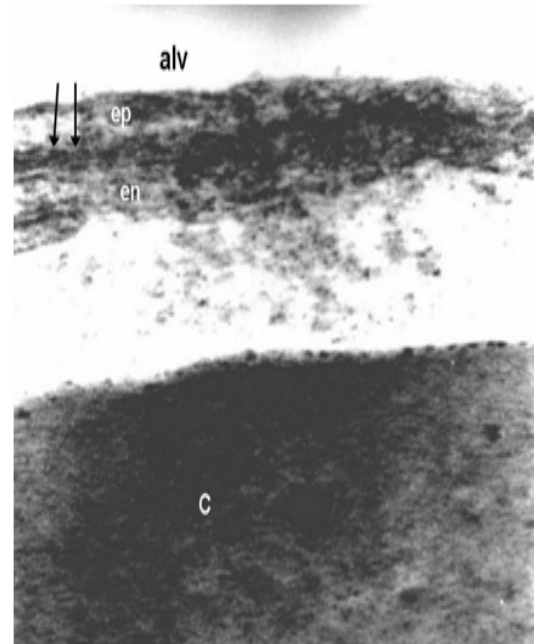


Fig. 8: An electron photomicrograph in the lung of a rat of the control group showing normal intact blood-air barrier formed from cytoplasm of type I pneumocyte (ep), cytoplasm of endothelial cells of capillary (en), fused basal lamina of pneumocyte type I and endothelial cells of capillary (arrow), alveolar space (alv) and red blood cell inside capillary lumen (C).
Uranyl acetate and Lead citrate; X 50,000

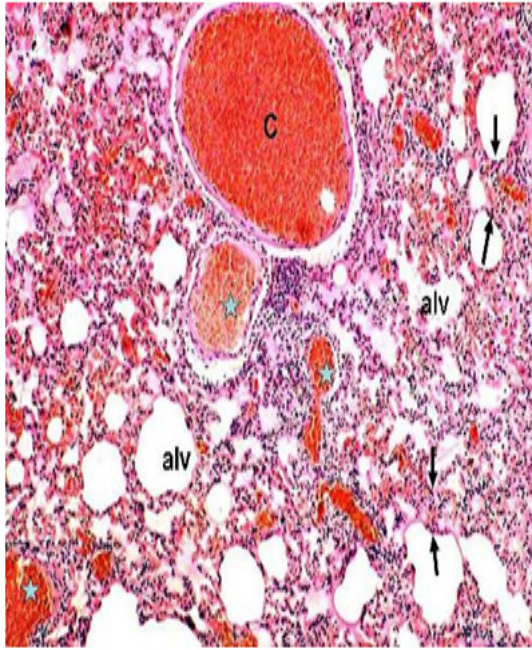


Fig. 9: A photomicrograph in the lung of a rat of carbon tetrachloride- treated group showing marked narrowing and occlusion of alveolar spaces (alv), marked increase in the thickness of interalveolar septa (arrow), congestion of blood vessels (C) and extravasation of blood into alveolar spaces (star). Hx.&E.; X400

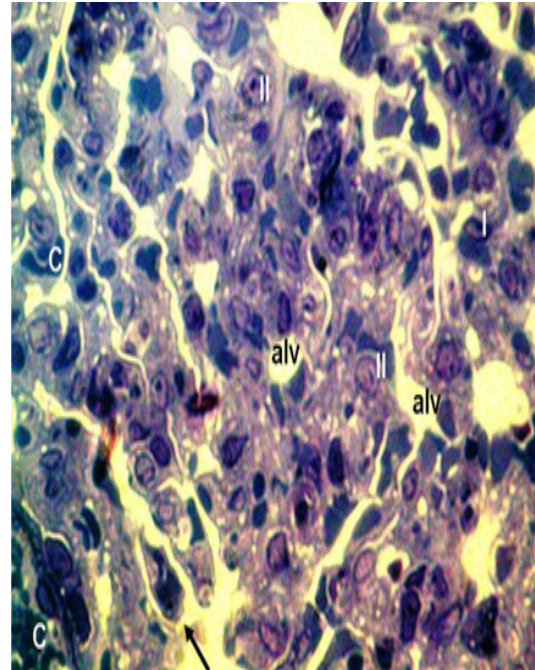


Fig. 11: A photomicrograph in the lung of a rat of carbon tetrachloride-treated group showing occlusion and narrowing of most alveolar space (alv), detached part of cell (arrow), hypocellularity of type I (I) and type II (II) pneumocytes and congested capillary (C). Toluidine blue; X 1000

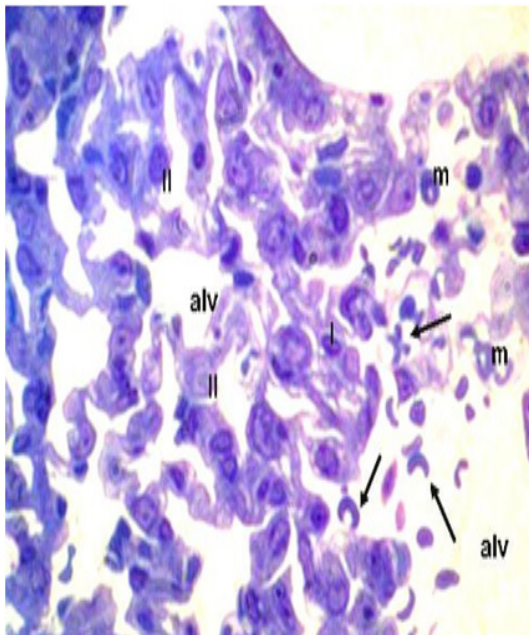


Fig. 10: A photomicrograph in the lung of a rat of the carbon tetrachloride-treated group showing extravasation of red blood cells into the alveolar space (arrows), hypocellularity of type I pneumocytes (I), lightly stained nucleus of type II pneumocytes (II) and alveolar macrophages (m) inside alveolar space (alv). Toluidine blue; X 1000

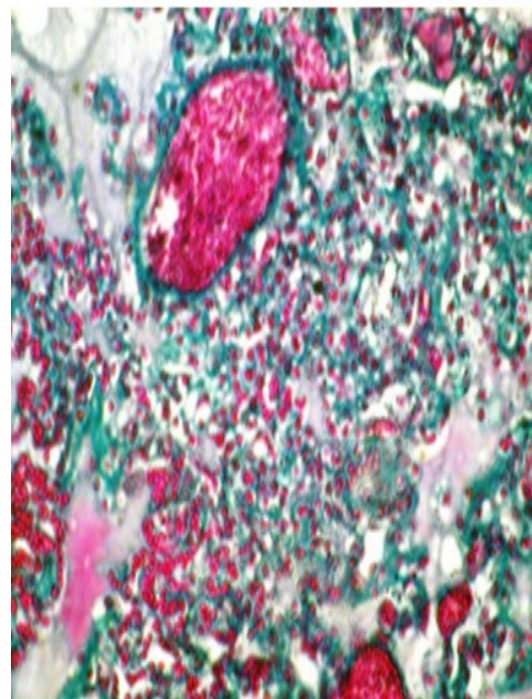


Fig. 12: A photomicrograph in the lung of a rat of carbon tetrachloride-treated group showing marked increase in the amount of green collagen fibers. Masson's trichrome; X400

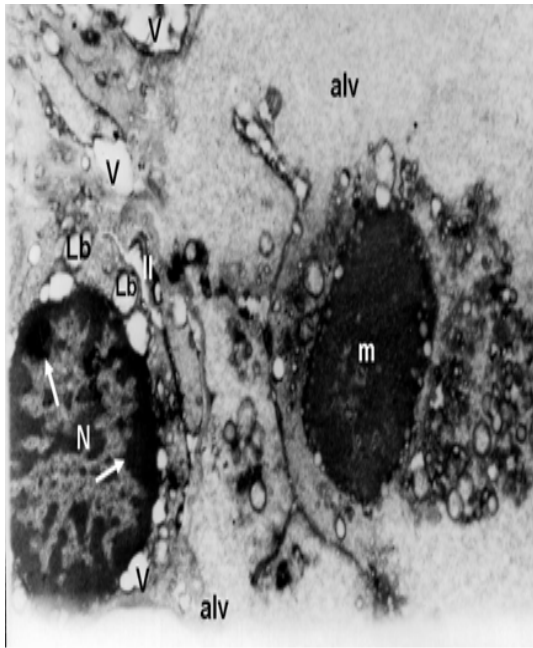


Fig. 13: An electron photomicrograph in the lung of a rat of carbon tetrachloride-treated group showing alveolar macrophage (m) inside alveolar space (alv), shrunk type II pneumocyte (II) with condensation of chromatin (arrows) inside the nucleus (N), multiple vacuations (V) and lamellar bodies (Lb).
Uranyl acetate and Lead citrate; X6,000

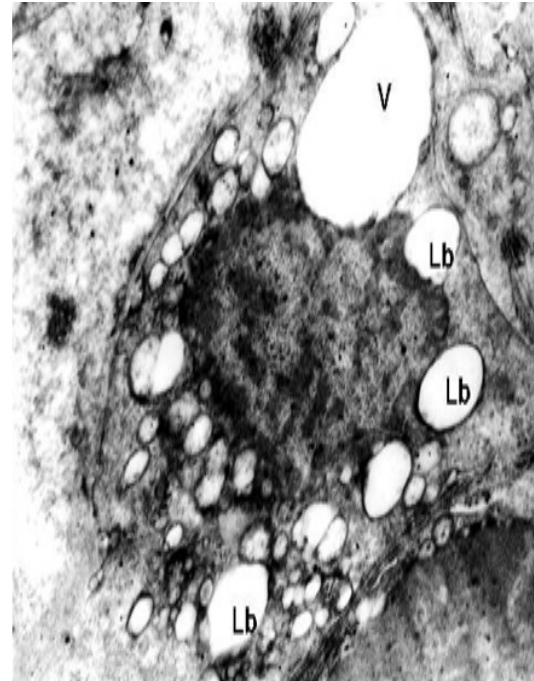


Fig. 15: An electron photomicrograph in the lung of a rat of carbon tetrachloride-treated group, showing type II pneumocytes with swelling of lamellar bodies (Lb) and vacuolation of the cytoplasm (V).
Uranyl acetate and Lead citrate; X10,000

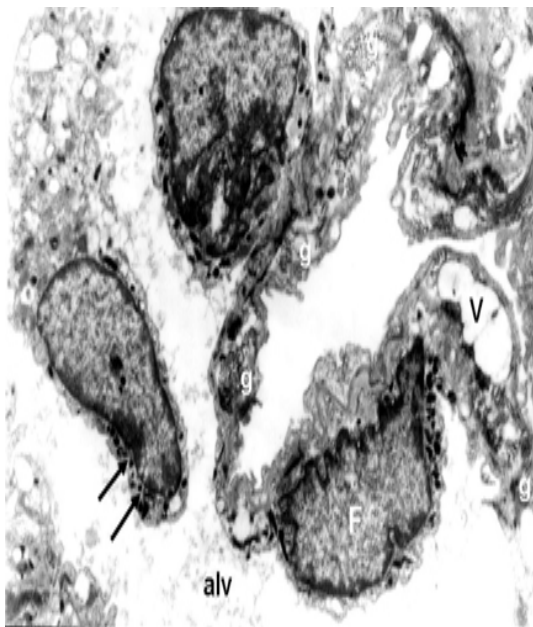


Fig. 14: An electron photomicrograph in the lung of a rat of carbon tetrachloride-treated group showing detached part of cell (arrow) inside alveolar space (alv), vacuolation of the cytoplasm (V), abundant amount of collagen fibers (g) and fibroblast (F).
Uranyl acetate and Lead citrate; X5,000



Fig. 16: An electron photomicrograph in the lung of a rat of carbon tetrachloride-treated group showing shrunk type II pneumocyte with condensation of the chromatin inside nucleus (N), multiple vacuations of the cytoplasm (V) and loss of tight junctions between cells (arrows).
Uranyl acetate and Lead citrate; X 5,000

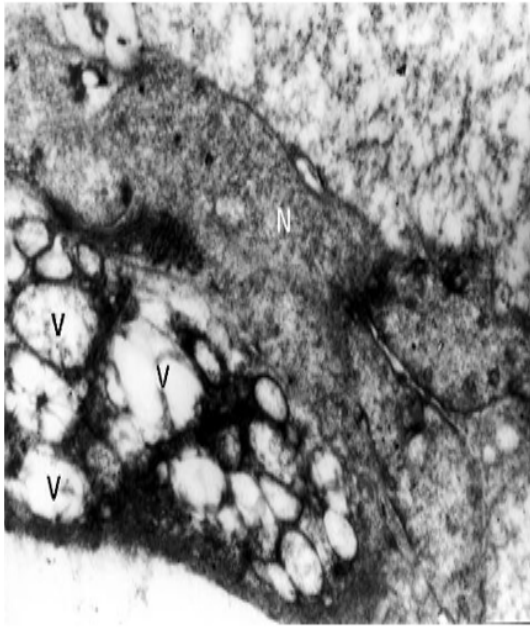


Fig. 17: An electron photomicrograph in the lung of a rat of carbon tetrachloride -treated group showing lightly stained nucleus of type I pneumocyte (N) and multiple vacuulations of the cytoplasm (V).
Uranyl acetate and Lead citrate; X10,000

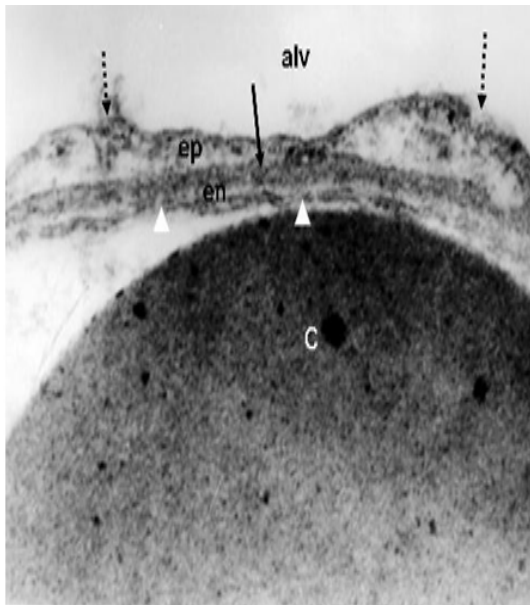


Fig. 18: An electron photomicrograph in the lung of a rat of carbon tetrachloride-treated group showing, rupture of blood-air barrier (dashed arrows) in the cytoplasm of type I pneumocyte (ep), discontinuation of the barrier (arrowheads) in the cytoplasm of endothelial cells of continuous capillary (en), separation of the two fused basal laminae of type I pueumocyte and endothelial cells of capillary (arrow), alveolar space (alv) and red blood cell inside capillary lumen (C).
Uranyl acetate and Lead citrate; X 50,000

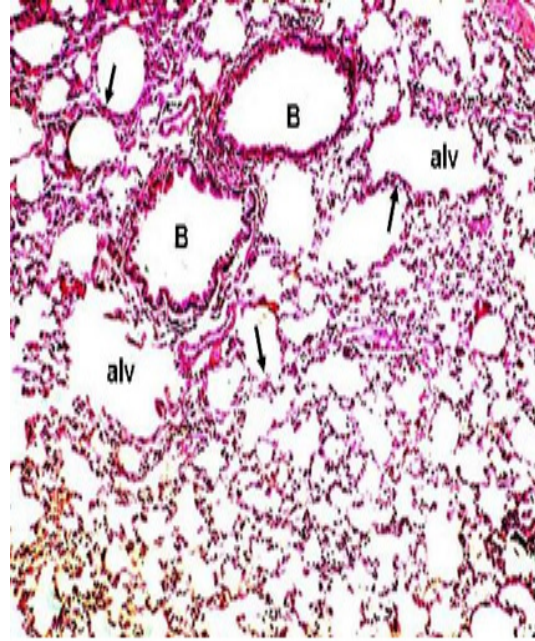


Fig. 19: A photomicrograph in the lung of a rat of G-CSF+carbon tetrachloride-treated group showing nearly a normal lung architecture. Note the alveolar space (alv), pulmonary bronchioles (B) and normal thickness of interalveolar septa (arrows).
Hx.&E.; X400

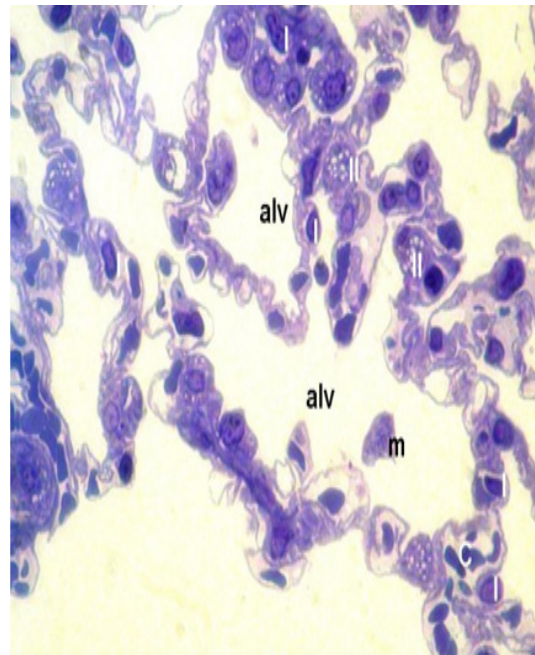


Fig. 20: A photomicrograph in the lung of a rat of G-CSF+carbon tetrachloride-treated group showing increase in number of type I pneumocytes (I), type II pneumocytes (II), alveolar space (alv), red blood cells inside capillary (C) and macrophage inside alveolar space (m).
Toluidine blue; X1000

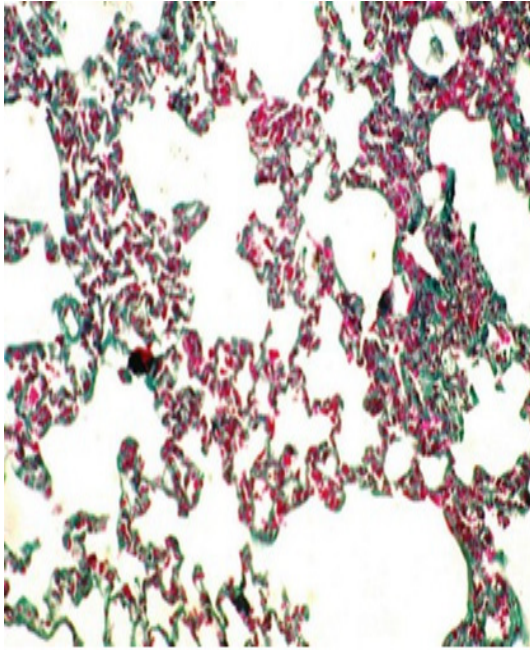


Fig. 21: A photomicrograph in the lung of a rat of G-CSF+carbon tetrachloride-treated group showing few amount of green collagen fibers in the interalveolar septa. Masson's trichrome ; X400

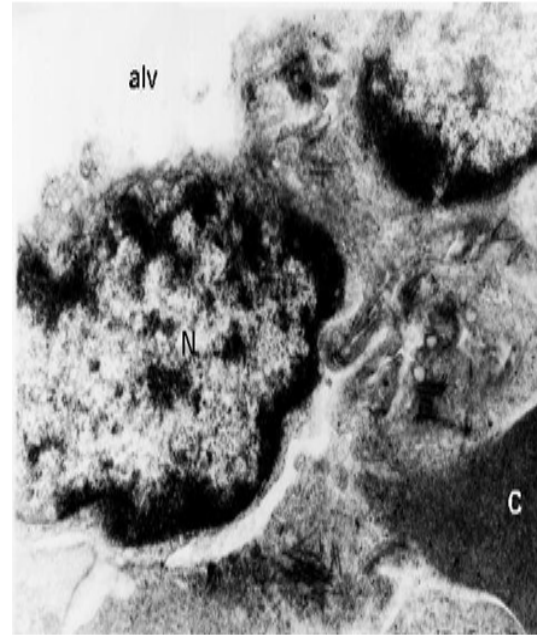


Fig. 23: An electron photomicrograph in the lung of a rat of G-CSF+carbon tetrachloride-treated group showing normal appearance of nucleus of type I pneumocyte (N), clear alveolar space (alv) and red blood cell inside capillary lumen (C). Uranyl acetate and Lead citrate; X10,000



Fig. 22: An electron photomicrograph of type II pneumocytes of adult lung tissue of a rat of G-CSF+carbon tetrachloride-treated group showing nearly normal appearance and size of lamellar body (Lb), normal appearance of nucleus (N) assuming normal microvilli (arrows). Uranyl acetate and Lead citrate; X10,000

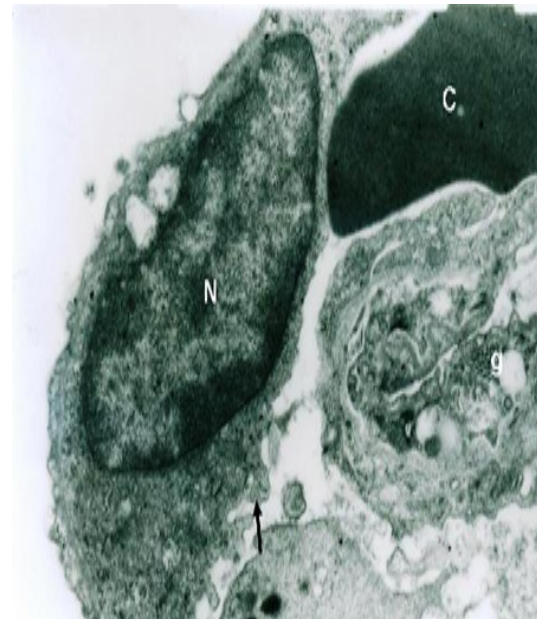


Fig. 24: An electron photomicrograph in the lung of a rat of G-CSF+carbon tetrachloride-treated group showing type II pneumocyte with features of turnover to type I pneumocytes. Note the flat nucleus (N) and losing microvilli (arrow). Note also red blood cell inside capillary lumen (c) and few amount of collagen fibers (g). Uranyl acetate and Lead citrate; X10,000

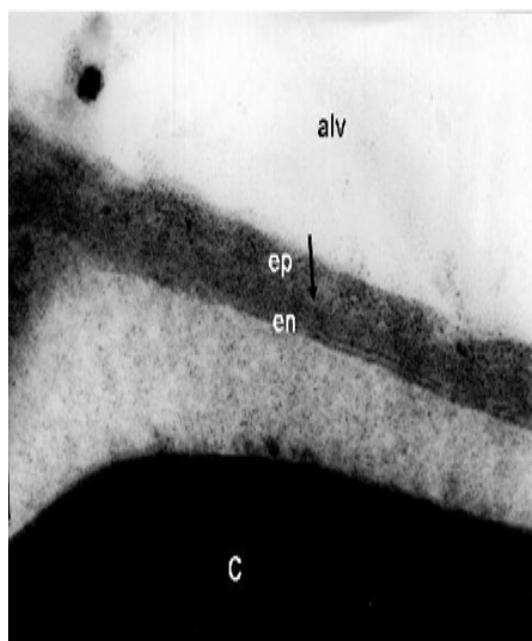


Fig. 25: An electron photomicrograph in the lung of a rat of G-CSF+carbon tetrachloride-treated group showing normal intact blood-air barrier formed of cytoplasm of type I pneumocyte (ep), cytoplasm of endothelial cells of continuous capillary (en), fused basal lamina of type I pneumocyte and endothelial cells of capillary (arrow) and red blood cell inside capillary lumen (C).
Uranyl acetate and Lead citrate; X 50,000

DISCUSSION

The lung specimens of the carbon tetrachloride-treated rats compared with those of the control ones showed congestion and rupture of most of the blood capillaries, marked thickening of the alveolar septa, marked narrowing, distortion and occlusion in most of the air spaces. A large number of inflammatory cells in the pulmonary tissue was also observed. Moreover, degenerated cells were detected in certain foci accompanied by obvious increase in the collagen fibers. These findings are in accordance with the results reported by *Paakko et al. (1996)* and *Zakareya et al. (2004)*. *Selman et al. (2001)* demonstrated that during homeostasis and in response to lung damage, type I pneumocytes are highly vulnerable to injury, while type II pneumocytes serve as progenitor cells as they are more resistant to injury and can therefore function as progenitor cells for regeneration of the alveolar epithelium. They explained that as these cells can proliferate and migrate to recover the denuded basement

membrane by forming a layer of cuboidal epithelial cells, they should differentiate to re-establish both type I and type II pneumocytes into a functional alveolar epithelium. This agrees with the results of the present study which revealed a highly statistically significant hypocellularity in both type I and II pneumocytes in carbon tetrachloride-treated group in comparison to both control and G-CSF+carbon tetrachloride-treated groups. Based on their explanation, the hypocellularity in type I pneumocytes, together with rupture of blood air barriers that were noticed in the present study in carbon tetrachloride-treated group, indicate that the proliferation and differentiation of type II pneumocytes were not quite enough to prevent either hypocellularity in type I cells or rupture of blood-air barriers under the effect of carbon tetrachloride. Moreover, this hypocellularity in both type I and II pneumocytes can reflect direct toxic effect of carbon tetrachloride administration on both types of pneumocytes. This effect appeared clearly in the pathological changes that were found in type II pneumocytes in the present study as most cells showed swelling, vacuulations of the cytoplasm, condensation of chromatin (inactive chromatin) and shrinkage in some other cells. It is therefore conceivable that carbon tetrachloride administration interfered with cell integration of both types of pneumocytes resulting in the pathogenesis of pulmonary fibrosis. *Cotran et al. (1994)* explained that the toxic effect of carbon tetrachloride is due to its conversion by cytochrome P450 to the highly reactive toxic free radical carbon trichloride (CCl₃). *VenKatesan et al. (1997)* added that these free radicals can damage nucleic acids, proteins, lipids and thus may contribute to the loss of enzymatic activity or structural integrity leading to increased trans-epithelial permeability and degeneration of cells.

Cross and Mercer (1993) mentioned that in the event of injury to the lung septa, fibroblasts, divide and secrete more collagen leading to overproduction of collagen and scarring, which interfere with gas exchange. Furthermore, *Selman et al. (2001)* proposed that pulmonary fibrosis probably results from multiple cycles of epithelial cell injury and activation that provoke the migration, proliferation and activation of mesenchy-

mal cells with the formation of active fibroblastic/ myofibroblastic foci leading to exaggerated accumulation of extracellular matrix and abnormal wound repair. This is in agreement with the results of the present study which revealed excessive increase in the amount of collagen fibers around the bronchioles and in the interalveolar septa in the carbon tetrachloride-treated groups in comparison to the control group.

Ishizawa et al. (2004) reported that bone marrow stem cells could be the source of progenitor cells for several cell types. They reported that mice with elastase-induced emphysema were treated with All-Trans Retinoic Acid (ATRA), Granulocyte Colony-Stimulating Factor (G-CSF), or a combination of both. ATRA or G-CSF promoted lung regeneration and increased bone marrow-derived cells in the alveoli. Their results indicate that bone marrow stem cells mobilization might be important in lung regeneration. Two more studies (*Yamada et al., 2004 & Rojas et al., 2005*) attempted to show that the normal repair of the lung relied on repair by circulating stem cells (from the bone marrow) as well as by local endogenous repair processes. They showed that secondary lung damage was increased if the bone marrow response was suppressed. Moreover, they added that this damage could be reversed if bone marrow stem cells were transplanted. Studies done by *Ortiz et al. (2003)*, *Ishizawa et al. (2004)* and *Rojas et al. (2005)* demonstrated that if the process of stem cell migration was augmented, lung injury could be reduced.

In the current study, treating rats with CCl₄ and GCS factor revealed that most of the main cell types of pulmonary tissue restored their normal histological and ultrastructural appearance as there were obvious increase in cellularity in both type I and type II pneumocytes and that both types of cells looked normal in most regions as compared to those of carbon tetrachloride-treated rats. This may reflect the promoting effect of G-CSF administration on lung regeneration through increasing bone marrow-derived stem cells in alveoli that ultimately induced proliferation of type II pneumocytes in an attempt to replace the damage in both type I and type II cells as mentioned by *Ishizawa et al. (2004)*. Meanwhile, these findings agree with the findings of *Summer et al. (2004)* which provided further support that adult lung cells could arise from the bone marrow. Moreover, *Reddy et al. (2004)* have suggested that type

II pneumocytes isolated from injured lungs could be segregated into at least two subpopulations: Type II responsible for repopulation and type II responsible for repair of damaged alveolar epithelium. Furthermore, turnover of type II to type I pneumocytes was observed in the current study. This is in compatible with *Guo et al. (2001)* who mentioned that differentiation of type II pneumocytes into type I pneumocytes is essential to re-establish a functional alveolar epithelium. This is supported by the study of *Koyama et al. (1998)* who explained that type II pneumocytes synthesize and secrete surfactant, control the volume and composition of the epithelial lining fluid and proliferate and differentiate into type I pneumocytes after lung injury to maintain the integrity of the alveolar wall. They added that type II pneumocytes have a role in modulating immunologic activity in the alveolar space as both in vivo and in vitro data suggest that type II pneumocytes could participate in the intra-alveolar cytokine network by secreting interleukin 8, interleukin 6 and monocyte chemoattractant protein.

On the other hand, our findings are contrary to those reported by *Azoulay et al. (2003)* and *Adachi et al. (2003)* who reported negative effect of G-CSF on lung injury induced by bleomycin. They explained that the exacerbating effects of G-CSF seemed to be associated with marked infiltration of the pulmonary tissue with activated neutrophils. Furthermore, other authors have suggested that the effects of neutrophils on the lung in the rats treated with G-CSF may be closely related not only to the number of neutrophils, but also to the inflammatory phase of the pulmonary lesions (*Adachi, 2002*). Moreover, *Adachi (2003)* added that the administration of G-CSF to rats with slight lung injury bearing no pulmonary fibrosis does not exacerbate the injury. The difference between his findings and ours may be due to the different underlying mechanisms of the causing agent of pulmonary fibrosis. Additionally, the difference in the results of the two experiments could result from the difference in the dose of G-CSF used in the two experiments. The used dose of G-CSF was sufficient to mobilize hematopoietic stem cells into the peripheral blood in adequate numbers but not causing lung injures. This explanation agrees with *Inano et al. (1998)* who indicated that injection of G-CSF caused rapid neutropenia and neutrophil sequestration in the lungs that is likely to be mediated through a G-CSF-induced decrease in neutrophil deformability. However, this G-CSF-induced

neutrophil sequestration did not appear to induce a massive lung injury.

In the present study the lung specimens of the carbon tetrachloride-treated rats revealed presence of excessive amounts of collagen fibers around the bronchioles, in the interalveolar septa and in the pulmonary blood vessels while in G-CSF+carbon tetrachloride-treated rats a minimal amount of collagen fibers was found. This is in agreement with the results of *Moodley et al. (2009)* who revealed that the collagen concentration in the lung was significantly reduced by stem cell treatment. Their results suggested that stem cells have antifibrotic properties and may augment lung repair. Also studies of *Plenz et al. (2003)* demonstrated that G-CSF plays a major role in the cytokine network regulating the metabolism of vascular collagens. They added that G-CSF deficiency leads to an altered composition of the vascular collagenous matrix, i.e., reduced amount of fibrillar collagen, altered ratio of fibrillar and network-forming collagen and failures in the fibrillogenesis suggesting that G-CSF is a basic requirement for the maintenance of vessel wall integrity and resilience.

In conclusion, there is evidence that bone marrow derived stem cells are able to target areas of the body undergoing injury and contribute to repair. The exact mechanisms are not wholly understood and different cell species may have different roles in certain situations.

REFERENCES

- Adach, K., Suzuki, M., Sugimoto, T., et al. 2002.* Granulocyte colony-stimulating factor exacerbates the acute lung injury and pulmonary fibrosis induced by intratracheal administration of bleomycin in rats. *Experimental and Toxicologic Pathology: Official Journal of the Gesellschaft Fur Toxikologische Pathologie* 53 (6): 501-510.
- Adachi, K., Suzuki, M., Sugimoto, T., et al. 2003.* Effects of granulocyte colony-stimulating factor (G-CSF) on bleomycin-induced lung injury of varying severity. *Toxicologic Pathology* 31 (6): 665-673.
- Azoulay, E., Herigault, S., Levame, M., et al. 2003.* Effect of granulocyte colony-stimulating factor on bleomycin-induced acute lung injury and pulmonary fibrosis. *Critical Care Medicine* 31 (5): 1442-1448.
- Blau, H. M., Brazelton, T. R. and Weimann, J. M. 2001.* The evolving concept of a stem cell: entity or function? *Cell* 105 (7): 829-841.
- Clark, S. C. and Kamen, R. 1987.* The human hematopoietic colony-stimulating factors. *Science* 236: 1229-1237.
- Cotran, R. S., Kumar, V. and Robbins, S. L. 1994.* Cellular injury and cellular death: in pathologic basis of disease. W.B. Saunders Co. U.S.A.
- Cross, P. C. and Mercer, K. L. 1993.* Cell and tissue ultrastructure: a functional perspective. NY, Freeman, New York.
- Edmonds, M., Bates, M., Doxford, M., et al. 2000.* New treatments in ulcer healing and wound infection. *Diabetes/Metabolism Research and Reviews* 16 (Suppl 1):51-54.
- Gough, A., Clapperton, M., Rolando, N., et al. 1997.* Randomised placebo-controlled trial of granulocyte-colony stimulating factor in diabetic foot infection. *Lancet* 350: 855-859.
- Gross, T. J. and Hunninghake, G. W. 2001.* Idiopathic pulmonary fibrosis. *The New England Journal of Medicine* 345 (7): 517-525.
- Guo, Y., Martinez Williams, C., Yellowley, C. E., et al. 2001.* Connexin expression by alveolar epithelial cells is regulated by extracellular matrix. *American Journal of Physiology. Lung Cellular and Molecular Physiology* 280 (2): 191-202.
- Koyama, S., Sato, E., Masubuchi, T., et al. 1998.* Alveolar type II-like cells release G-CSF as neutrophil chemotactic activity. *The American Journal of Physiology* 275 4 (1): 687-693.
- Hartung, T. 1999.* Immunomodulation by colony-stimulating factors. *Reviews of Physiology, Biochemistry and Pharmacology* 136: 1-164.
- Inano, H., Kameyama, S., Yasui, S. and Nagai, A. 1998.* Granulocyte colony-stimulating factor induces neutrophil sequestration in rabbit lungs. *American Journal of Respiratory Cell and Molecular Biology*: (1): 167-174.

- Ishizawa, K., Kubo, H., Yamada, M., et al. 2004.** Bone marrow-derived cells contribute to lung regeneration after elastase-induced pulmonary emphysema. *FEBS Letters* 556 (1-3): 249-252.
- Loebinger, M. R. and Janes, S. M. 2007.** Stem cells for lung disease. *Chest* 132 (1): 279-285.
- Mason, R. J., Schwarz, M. I., Hunninghake, G. W. and Musson, R. A. 1999.** NHLBI Workshop Summary. Pharmacological therapy for idiopathic pulmonary fibrosis. Past, present and future. *American Journal of Respiratory and Critical Care Medicine*. 160 5 (1): 1771-1777.
- Mehrnaz, G.K., Gyetko, M. R., Hu, B. and Phan, S. H. 2007.** New insights into the pathogenesis and treatment of idiopathic pulmonary fibrosis: a potential role for stem cells in the lung parenchyma and implications for therapy. *Pharmaceutical Research* 24 (5): 819-841.
- Moodley, Y., Atienza, D., Manuelpillai, U., et al. 2009.** Human umbilical cord mesenchymal stem cells reduce fibrosis of bleomycin-induced lung injury. *American Journal of Pathology* 175 (1): 303-313.
- Orlic, D., Kajstura, J., Chimenti, S., et al. 2001.** Mobilized bone marrow cells repair the infarcted heart, improving function and survival. *Proceedings of the National Academy of Sciences of the United States of America* 98 (18): 10344-10349.
- Ortiz, L. A., Gambelli, F., McBride, C., et al. 2003.** Mesenchymal stem cell engraftment in lung is enhanced in response to bleomycin exposure and ameliorates its fibrotic effects. *Proceedings of the National Academy of Sciences of the United States of America* 100 (14): 8407-8411.
- Paakko, P., Anttila, S., Sormunen, R., et al. 1996.** Biochemical and morphological characterization of carbon tetrachloride-induced lung fibrosis in rats. *Archives of Toxicology* 70 (9): 540-552.
- Plenz, G., Eschert, H., Beissert, S., et al. 2003.** Alterations in the vascular extracellular matrix of granulocyte macrophage colony-stimulating factor (GM-CSF) -deficient mice. The FASEB Journal official Publication of the Federation of American Societies for Experimental Biology 17 (11): 1451-1457.
- Reddy, R., Buckley, S., Doerken, M., et al. 2004.** Isolation of a putative progenitor subpopulation of alveolar epithelial type 2 cells. *American Journal of Physiology, Lung Cellular and Molecular Physiology* 286 (4): 658-667.
- Rojas, M., Xu, J., Woods, C. R., et al. 2005.** Bone marrow-derived mesenchymal stem cells in repair of the injured lung. *American Journal of Respiratory Cell and Molecular Biology*: 33 (2): 145-152.
- Sehara, Y., Hayashi, T., Deguchi, K., et al. 2007.** G-CSF enhances stem cell proliferation in rat hippocampus after transient middle cerebral artery occlusion. *Neuroscience Letters* 418 (3): 248-252.
- Selman, M., King, T. E. and Pardo, A. 2001.** Idiopathic pulmonary fibrosis: prevailing and evolving hypotheses about its pathogenesis and implications for therapy. *Annals of Internal Medicine* 134 (2): 136-151.
- Summer, R., Kotton, D. N., Sun, X., et al. 2004.** Translational physiology: origin and phenotype of lung side population cells. *American Journal of Physiology, Lung Cellular and Molecular Physiology* 287 (3): L477-483.
- Taylor, M. D., Roberts, J. R., Hubbs, A. F., et al. 2002.** Quantitative image analysis of drug-induced lung fibrosis using laser scanning confocal microscopy. *Toxicological Sciences, Life Sciences* 61 (6): 51-58.
- Venkatesan, N., Punithavathi, V. and Chandrakasan, G. 1997.** Curcumin protects bleomycin-induced lung injury in rats. *Life Sciences* 61 (6): PL51-58.
- Weaver, C. H., Buckner, C. D., Longin, K., et al. 1993.** Syngeneic transplantation with peripheral blood mononuclear cells collected after the administration of recombinant human granulocyte colony-stimulating factor. *Blood* 82 (7): 1981-1984.
- Yamada, M., Kubo, H., Kobayashi, S., et al. 2004.** Bone marrow-derived progenitor cells are important for lung repair after lipopolysaccharide-induced lung injury. *Journal of Immunology (Baltimore)* 172 (2): 1266-1272.
- Zakareya, E., Abdel-Khaleq, E. and Selim, M. E. 2004.** The protective role of curcumin against carbon tetrachloride-induced pulmonary injury in rats. *Egyptian Journal of Medical Laboratory Sciences* 17 (2): 83-99.
- Zhang, H. Q., Yau, Y. F., Szeto, K. Y., et al. 2007.** Therapeutic effect of Chinese medicine formula DSQRL on experimental pulmonary fibrosis. *Journal of Ethnopharmacology* 109 (3): 543-546.

دراسة بالمجهر الضوئي و المجهر الالكتروني عن دور العلاج بالعامل المحفز (Granulocyte Colony Stimulating Factor) فى التليف الرئوى الناتج عن مادة رابع كلوريد الكربون فى ذكور الفئران البيضاء البالغة

منى حسن محمد على ، أميمة محفوظ محمود ، نرمين سمير نصير ، هالة محمد عبيد*
قسم التشريح- كلية الطب البشرى و قسم علم الحيوان * - كلية العلوم- جامعة قناة السويس

ملخص البحث

التليف الرئوي هو شكل خطير قاتل من أمراض الرئة التي لا يوجد لها علاج فعال. في الآونة الأخيرة لوحظ انه يمكن ان يكون للخلايا الجذعية الدموية المنشأ دور فى علاج الاعضاء غير دموية المنشأ ومن ثم تم الاعتقاد بإمكانية مساهمتها فى علاج هذه الاعضاء.

الهدف من الدراسة : اختبار ما إذا كان العامل المحفز (Granulocyte Colony Stimulating Factor) يمكن أن يعزز و يساهم فى إصلاح التليف الرئوى الناتج عن مادة رابع كلوريد الكربون فى ذكور الفئران البيضاء البالغة.

طرق البحث : تم استخدام عدد ثمانين ذكر فأر ابيض بالغ و قسمت عشوائيا إلى أربع مجموعات : مجموعة (١) هى المجموعة الضابطة ، مجموعة (٢) : معالجة بمادة رابع كلوريد الكربون حيث تم حقن الفئران فى الغشاء البريتونى بجرعة مقدارها 6٠0 مليجرام | كج من وزن الجسم يوميا لمدة ١٤ يوما متتاليا ومن ثم قسمت الى مجموعتين : مجموعة (أ): حيث تمت التضحية بالحيوانات بعد ٢٤ ساعة من نهاية الحقن ومجموعة (ب): حيث تمت التضحية بالحيوانات بعد ١٤ يوما من نهاية الحقن. المجموعة (٣) : معالجة بمادة رابع كلوريد الكربون بالإضافة الى العامل المحفز (Granulocyte Colony Stimulating Factor) حيث تم حقن الحيوانات بمادة رابع كلوريد الكربون فى الغشاء البريتونى بجرعة مقدارها 6٠0 مليجرام | كج من وزن الجسم يوميا لمدة ١٤ يوما متتاليا ثم تلاها الحقن بالعامل المحفز

(Neupogen) (Granulocyte Colony Stimulating Factor) بجرعة مقدارها ١٠٠ ميكروجرام / كج / يوم لمدة 5 أيام متتالية تحت الجلد وتمت التضحية بالحيوانات بعد ١٤ يوما من نهاية الحقن. المجموعة (٤) : معالجة بالعامل المحفز (Granulocyte Colony Stimulating Factor) حيث تم حقن الحيوانات بالعامل المحفز (Neupogen) (Granulocyte Colony Stimulating Factor) بجرعة (١٠٠ ميكروجرام / كج / يوم) تحت الجلد لمدة ٥ أيام متتالية وتمت التضحية بالحيوانات بعد ١٤ يوما من نهاية الحقن. وقد تم أخذ عينات من الرئة و تحضيرها و صبغها و فحصها بالمجهرين الضوئى والالكترونى.

النتائج : وجد أن رئة الفئران المعالجة بمادة رابع كلوريد الكربون قد أظهرت احتقان واسع وتمزق معظم الشعيرات الدموية و ازدياد سمك الحاجز السنخي و ضيق ملحوظ وانسداد في معظم الحويصلات الهوائية مع وجود عدد كبير من الخلايا الالتهابية في النسيج الرئوي. هذا بالإضافة الى زيادة واضحة في ألياف الكولاجين. وكشفت النتائج التي تم الحصول عليها من مجموعة من الفئران المعالجة بمادة رابع كلوريد الكربون مع العامل المحفز (Granulocyte Colony Stimulating Factor) انخفاض ملحوظ في التغيرات المرضية في الرئتين.

الخلاصة : على الرغم من أنه ليس مفهوما كليا الآليات الدقيقة فان هناك أدلة على أن الخلايا الجذعية المستمدة من نخاع العظام قادرة على المساهمة فى تعزيز الشفاء من التليف الرئوى.